Evaluation of Quasi-Static Matrix Parameters for Multiconductor Transmission Lines Using Galerkin's Method

Miodrag B. Baždar, Antonije R. Djordjević, Roger F. Harrington, *Life Fellow, IEEE,* and Tapan K. Sarkar, *Fellow, IEEE*

***Abstract*— Quasi-static matrix parameters for multiconductor transmission lines are numerically evaluated by solving a set of integral equations for the bound charges using Galerkin's technique, with a piecewise constant approximation for the charge distribution. Several hints are given as how to improve the efficiency and accuracy of computations.**

I. Introduction

With the increased speed of digital computers, much attention has been given to coupled transmission lines (multiconductor transmission lines). For most applications in evaluating transients on these lines a quasi-static analysis is sufficient [1]. This analysis is also sufficient for many applications in the analysis and design of microwave circuits, although in many other cases more complicated models, which take into account the dispersion as well as radiation, are required [2].

Various papers have been published dealing with the numerical evaluation of quasi-static matrix parameters of multiconductor transmission lines. Many of them are specialized to planar (printed) circuits, while fewer deal with structures of arbitrary cross sections. Our major interest is in the latter techniques, which can be divided into two groups: volume-formulation and surface-formulation. In the first group, the numerical solution involves the field quantities within the whole volume of the transmission line dielectrics (finite elements, finite differences, integral equations for volume bound charges). These techniques are most general, and they can easily handle arbitrary inhomogeneous dielectrics. The surface-formulation methods (also referred to as boundary-element techniques) involve only quantities at surfaces of material discontinuities, and are thus suitable for piecewise-homogeneous media. According to our experience, the integral equation formulations are superior in performance over finite-element and finite-difference formulations, and also for most practical purposes the medium is piecewise-homogeneous. Therefore, we will concentrate on the surface-formulation methods, which have been extensively covered in the literature [3]–[6]. The major aim of this paper is to present some recent improvements in these techniques [7], which resulted in a better efficiency of the computer programs and in improved accuracy of the results.

Manuscript received April 14, 1993; revised September 27, 1993.

M. B. Baždar is with the Institute of Microwave Techniques and Electronics, P.O. Box 58, 11071 Belgrade, Yugoslavia.

A. R. Djordjević is with the School of Electrical Engineering, University of Belgrade, P.O. Box 816, 11001 Belgrade, Yugoslavia.

R. F. Harrington and T. K. Sarkar are with the Department of Electrical and Computer Engineering, Syracuse University, Syracuse, N.Y. 13244-1240.

II. Outline of the Method

We assume the transmission line to have N signal conductors and one reference ("ground") conductor, that it is uniform along its length, and that its dielectric is piecewise homogeneous. The primary quasi-static parameters of this line are the matrix of inductances per unit length $[L']$, the matrix of electrostatic induction coefficients per unit length $[B']$, the matrix of resistances per unit length $[R']$, and the matrix of conductances per unit length $[G']$. In a quasi-static analysis, assuming the skin-effect to be fully pronounced, the matrices $[B']$ and $[G']$ are evaluated from the solution to one electrostatic problem, while the matrices $[L']$ and $[R']$ are evaluated from the solution to another electrostatic problem. The first electrostatic problem is the analysis of a two-dimensional system which coincides with the analyzed multiconductor transmission line. The dielectric losses are evaluated by taking the dielectric permittivity to be complex, and the analysis results in a complex matrix of electrostatic induction coefficients from which the required real matrices $[B']$ and $[G']$ are obtained. If the dielectrics are nonmagnetic, the second electrostatic problem consists of only the transmission-line conductors while the dielectrics are removed and replaced by a vacuum. The solution of this problem results in the matrix $[B'_o]$, and $[L'] = (1/c_o^2)[B'_o]^{-1}$, where $c_o = 1/\sqrt{\epsilon_o \mu_o}$. Using the perturbation approach, the matrix $[B']$ can be evaluated from this solution. (In the case where the material is magnetic, but linear, the evaluation of the matrix $[L']$ can be reduced to an analysis of an equivalent electrostatic system where the relative dielectric permittivity is taken to be $\epsilon_{re} = 1/\mu_r$, as explained in [8].)

In the analysis of the above two electrostatic systems, the conductors are replaced by their free surface charges (of density ρ_s), and the dielectrics by their bound surface charges (of density ρ_{sb}), located in vacuum. These two charges are considered together as the total charge of density $\rho_{st} = \rho_s + \rho_{sb}$, which are sources of the potential and the electric field.

Setting the potential $V(\vec{r})$ at a conductor surface equal to the corresponding conductor potential, a set of integral equations is obtained for the total charges. Another set of integral equations is obtained from the boundary conditions

for the normal electric field in the original system (with dielectrics), and in the equivalent system (dielectrics replaced by bound charges). More details about these integral equations can be found in [3]–[6]. These integral equations are solved numerically, using the method of moments [9]. As in [3]–[6], we use a piecewise-constant (pulse) approximation for the total charges. To that purpose, we approximate the contours of conductor-to-dielectric and dielectric-to-dielectric interfaces by a total of N_t chained straight-line segments (each of the segments corresponds to a flat, thin strip), and assume the charge distribution to be uniform along a segment. This amounts to defining a set of expansion functions

$$f_i(\vec{r}) = \begin{cases} 1 & \text{along } i\text{th segment} \\ 0 & \text{elsewhere} \end{cases}, \tag{1}$$

so that

$$\rho_{st}(\vec{r}) \approx \sum_{i=1}^{N_t} \rho_{sti} f_i(\vec{r}), \tag{2}$$

where ρ_{sti} are unknown constants to be solved for, and $\vec{r}$ is the position vector. However, instead of the point-matching technique used in [3]–[6], we now use Galerkin's method, which generally results in a smaller overall number of unknowns for a given accuracy, and thus in a more efficient computer program. This technique amounts to using functions (1) for testing as well as expansion. The equations obtained from the boundary conditions for the potential and for the electric fields finally yield the following system of linear equations in ρ_{sti}:

$$\sum_{i=1}^{N_t} \frac{\rho_{sti}}{2\pi\epsilon_o} \int_{c_j}\int_{c_i} \log\frac{k}{|\vec{r}-\vec{r}'|} dl'\, dl = V_j l_j, \qquad j = 1, \cdots, N_c, \tag{3}$$

$$(\epsilon_{r1}-\epsilon_{r2}) \sum_{\substack{i=1 \\ i\neq j}}^{N_t} \frac{\rho_{sti}}{2\pi\epsilon_o} \int_{c_j}\int_{c_i} \frac{(\vec{r}-\vec{r}')\cdot\vec{n}}{|\vec{r}-\vec{r}'|^2} dl'\, dl - \frac{\epsilon_{r1}+\epsilon_{r2}}{2\epsilon_o}\rho_{stj} l_j = 0, \qquad j = N_c+1, \cdots, N_t, \tag{4}$$

where $\vec{r}$ is the position of the field point, $\vec{r}'$ is the position of the source point, dl' is an element of the source segment (c_i), dl is an element of the field segment (c_j), K is an arbitrary constant, ϵ_{r1} and ϵ_{r2} are relative permittivities of the dielectrics at the two sides of the field segment, $\vec{n}$ is a unit normal directed from the second towards the first dielectric, N_c is the total number of segments for the conductors, and l_j is the length of the jth segment. The closed forms for the integrals in the above equations are given in the appendix. The potential integrals in (3) are identical when i and j are interchanged, and the Cartesian components of the electric-field integrals (with respect to a global coordinate system) in (4) differ only in the sign. Noting these symmetries, the computation time for the matrix elements can be reduced by almost a factor of two.

When we analyze a system with an infinite ground plane, we account for the influence of the plane by images of the total charges. Hence, the net charge of the system is zero, and the constant K is eliminated. When we analyze a system with a finite ground plane, we must impose the condition that the net charge of the system is zero,

$$\sum_{i=1}^{N_t} \rho_{sti} l_i = 0, \tag{5}$$

in order to obtain a finite energy per unit length. With this condition the constant K is again eliminated, so that, formally, we can take in (3) the Green's function for the potential to be $-\log|\vec{r}-\vec{r}'|$ instead of $\log(K/|\leq \vec{r}-\vec{r}'|)$. In addition, in this case we must not arbitrarily specify the potentials of all $(N+1)$ conductors, but only N voltages between the signal conductors and the reference conductor. We bypass this problem by dividing each of equations (3) by l_j, subtracting the last of (3) (for $j = N_c$, which corresponds to the last segment on the reference conductor) from all the previous equations (thus obtaining the voltages between the signal conductors and the reference conductor on the right-hand sides), and replacing the equation for $j = N_c$ by (5).

Once the total surface charges are found, it is necessary to find the free charges on the conductor surfaces. For a finite-thickness conductor, embedded in a dielectric of relative permittivity ϵ_r, we have simply $\rho_s = \epsilon_r \rho_{st}$. However, for an infinitesimally thin conductor the density of the free charge is evaluated from the boundary condition for the normal component of the electric field, as explained in [6].

The conductors of the second electrostatic system (for the evaluation of the matrices $[L']$ and $[R']$) coincide with the conductors of the first system (for the evaluation of the matrices $[B']$ and $[G']$). If identical segmentations are used in both cases, then for the second system only (3) is to be solved, for $i = 1, \cdots, N_c$. Hence, the matrix of the system of linear equations for the second electrostatic system is a submatrix of the corresponding matrix for the first electrostatic system. The two systems of linear equations can be solved simultaneously, taking care about the pivotization, so that the solution of the second electrostatic system requires very little additional computational time after solution of the first system.

The evaluation of the matrix $[R']$ is based on the solution of the second electrostatic system. Knowing the free-charge distribution, we obtain the surface-current density by $J_s = c_o \rho_s$, and the power loss (in conductors) per unit length by

$$P_c' = \int_{C_c} R_s J_s^2\, dl, \tag{6}$$

where R_s is the surface resistance of the conductors, and C_c denotes the contours of all conductors. Note that for infinitesimally thin conductors we must separate the current densities at both faces. Although the perturbation technique breaks down in this case because it theoretically gives infinite losses due to the edge effect, numerical results still give reasonable results for losses due to the approximation of the charge distribution. On the other hand, we have

$$P_c' = \sum_{m=1}^{N}\sum_{n=1}^{N} R'_{mn} I_m I_n, \tag{7}$$

where R'_{mn} are elements of the matrix $[R']$, and I_m is the current of the mth signal conductor. We start with the case when $I_1 = 1$ A, while all the other currents are zero, when $P'_c = R'_{11}I_1^2$, and evaluate R'_{11}. We repeat this procedure for all the other signal conductors to evaluate R'_{mm} $(m = 2, \cdots, N)$. Next, we take $I_1 = I_2 = 1$ A, and all the other currents to be zero. Now, $P'_c = R'_{11}I_1^2 + 2R'_{12}I_1I_2 + R'_{22}I_2^2$ (because $R'_{12} = R'_{21}$), and we evaluate R'_{12}. Finally, we repeat the procedure for all the other pairs of I_m and I_n to obtain the remaining elements of the matrix $[R']$.

III. Distribution of Pulses

The pulse approximation is probably the simplest, but crudest, approximation of the charge distribution. It can accommodate an arbitrary geometry, but it may not give the most accurate and efficient solutions. In many cases a more sophisticated approximation may be advantageous, such as a smooth approximation function along those parts of conductors where the charge distribution is expected to be smooth, and an inclusion of edge-effect terms. In addition to the approximation of the charge distribution, the pulse approximation, as applied here, involves an approximation of the geometry. For example, a circular cross section of a conductor is approximated by a polygonal line. This can be a problem, for example, when the conductor is placed close to a ground plane, and a relatively large number of pulses is required to properly model the geometry. In such cases, a curvilinear approximation of the conductor and dielectric contours may be advantageous. If, however, straight-line pulses are used for a circular conductor, it is useful to take the pulses so that the polygon they form is midway between an inscribed and a circumscribed polygon.

In order to increase the accuracy of the modeling with pulses, and to improve the efficiency of computations, it is advisable to take the pulses smaller in the region where the charge density is expected to have more rapid variations, such as near edges or wedges of a conductor or a dielectric. For example, the charge density of an infinitely thin strip of width $2a$ which is located far away from other objects is given by $\rho_s(x) = \rho_s(0)/\sqrt{a^2 - x^2}$, where x is a local coordinate running along the strip width $(-a < x < a)$. For this case it was found by numerical experiments [10] that a good strategy was to adopt a pulse distribution such that the total charge on each pulse was the same. If N pulses are taken for this strip, then the end points of the pulses are determined by $x_i = -a\cos(i\pi/N)$, $i = 0, \cdots, N$. This scheme can also be applied when the strip is close to other objects, although better segmentation schemes can be designed. Similar reasoning can be applied for conductor and dielectric wedges, where appropriate analytical expressions for the field could be taken (for example, from [11]). Concerning the complete structure to be analyzed, pulses should have shorter lengths in regions where the charges suffer rapid changes. Pulses should be longer in regions where the charges are relatively uniformly distributed, and where the absolute value of the charge density is expected to be small. However, since the actual field may not be easily estimated, a simple policy may be to take the shortest pulses to have approximately the same lengths for all parts of the structure. Based on this rule, automatic segmentation procedures can be designed for many structures.

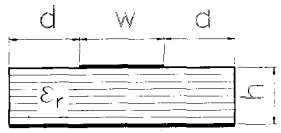

Fig. 1. Sketch of a microstrip line.

In some cases, an infinite ground plane is modeled by a finite-width plane because it may be computationally advantageous. For example, if a complex structure with several dielectric layers and/or finite-width conductors (requiring a lot of unknowns) is placed close to a ground plane, and if the image theory is applied, the number of basic integrals equals twice the number of unknowns, because of the image contribution. If, however, a finite-width ground plane is used, the total number of unknowns is increased, but this increase may be marginal compared to the total number of unknowns (because the structure is complex), resulting in a much smaller number of basic integrals which are to be evaluated. In the case of two ground planes, if infinitely wide planes are used, Green's function becomes very hard for numerical evaluation, which can significantly increase the computation time. Taking finite-width planes can be advantageous in such cases, since it yields good results even with very narrow planes, as demonstrated later.

In such cases, the question arises about the required minimal width. To estimate this width, consider a microstrip line (Fig. 1) with an infinite ground plane. The field produced by the signal conductor and its image in the ground plane, in the absence of the dielectric, behaves like a field of a line dipole which decays as $1/r^2$, where r is the distance from the strip. As a consequence, the density surface charge induced in the ground plane also decays as $1/r^2$. By truncating the ground plane at a distance r from the strip, we may expect the error to decay slower than $1/r^2$. Numerical experiments have shown that this error is of the order of $1/r$, and to achieve an error of about 1% in the capacitance or inductance it suffices to take the ground plane to extend about $5h$ on either side of the strip, where h is the substrate thickness. In the case of two parallel ground planes, such as for a stripline structure (Fig. 2), the field decays exponentially away from the strip (like that of a waveguide mode below cutoff). For a symmetrically positioned strip, the field decays as $\exp(-\pi r/H)$, where r is the distance from the strip and H the distance between the ground planes. For an 1% error the finite ground planes should extend about a distance H on either side of the strip.

IV. Numerical Examples

First, we compare the accuracy of Galerkin's and point-matching solutions, and of nonuniform and uniform segmentations. Presented in Table I are results for inductance per unit length (L'), capacitance per unit length (C'), characteristic impedance (Z_c), and effective relative permittivity (ϵ_{re}) of the microstrip line sketched in Fig. 1, versus the numbers of

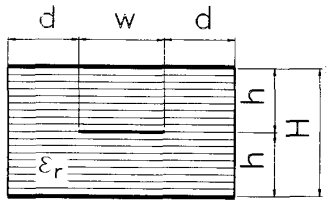

Fig. 2. Sketch of a stripline.

TABLE I
INDUCTANCE PER UNIT LENGTH (L'), CAPACITANCE PER UNIT LENGTH (C'), CHARACTERISTIC IMPEDANCE (Z_c), EFFECTIVE RELATIVE PERMITTIVITY (ϵ_{re}), AND CPU TIME (t_1 FOR EVALUATING THE MATRIX ELEMENTS, AND t_2 FOR SOLVING THE SYSTEM OF LINEAR EQUATIONS) FOR THE MICROSTRIP LINE OF FIG. 1 WITH $w = 2$ mm, $h = 1$ mm, $\epsilon_r = 4$, AND $d = 5$ mm, VERSUS THE NUMBERS OF SEGMENTS FOR THE STRIP (N_w) AND EACH UPPER SURFACE OF THE DIELECTRIC (N_d), FOR GALERKIN'S TECHNIQUE (GAL), POINT-MATCHING METHOD (PM), NONUNIFORM SEGMENTATION (NUS), AND UNIFORM SEGMENTATION (US)

N_w	N_d	method	L' [nH/m]	C' [pF/m]	Z_c [Ω]	ϵ_{re}	t_1 [s]	t_2 [s]
1	1	GAL/NUS	314.2	108.2	53.87	3.056	0.05	0.00
		GAL/US	314.2	108.2	53.87	3.056	0.05	0.00
		PM/NUS	345.6	95.97	60.01	2.981	0.03	0.00
		PM/US	345.6	95.97	60.01	2.981	0.03	0.00
2	2	GAL/NUS	314.2	108.2	53.87	3.056	0.11	0.00
		GAL/US	314.2	108.2	53.87	3.056	0.11	0.00
		PM/NUS	324.7	103.1	56.12	3.010	0.07	0.00
		PM/US	324.7	103.1	56.12	3.010	0.07	0.00
4	4	GAL/NUS	302.4	113.4	51.64	3.082	0.33	0.05
		GAL/US	305.9	112.1	52.25	3.081	0.33	0.05
		PM/NUS	305.4	111.2	52.40	3.052	0.21	0.05
		PM/US	311.1	108.8	53.49	3.042	0.21	0.05
8	8	GAL/NUS	298.4	114.8	50.98	3.080	1.05	0.16
		GAL/US	301.6	113.6	51.54	3.078	1.05	0.16
		PM/NUS	299.2	114.0	51.24	3.065	0.71	0.16
		PM/US	302.4	111.9	51.14	3.057	0.71	0.16
16	16	GAL/NUS	297.4	115.1	50.82	3.077	3.73	1.10
		GAL/US	299.3	114.3	51.18	3.075	3.73	1.10
		PM/NUS	297.5	114.8	50.91	3.069	2.47	1.10
		PM/US	300.6	113.4	51.47	3.064	2.47	1.10
32	32	GAL/NUS	297.1	115.1	50.80	3.074	14.01	7.91
		GAL/US	298.2	114.3	50.99	3.073	14.01	7.91
		PM/NUS	297.1	115.0	50.83	3.070	9.56	7.91
		PM/US	298.8	114.2	51.14	3.068	9.56	7.91
64	64	GAL/NUS	297.0	115.1	50.80	3.072	54.10	60.52
		GAL/US	297.6	114.9	50.90	3.072	54.10	60.52
		PM/NUS	297.0	115.0	50.81	3.071	37.52	60.52
		PM/US	297.9	114.6	51.97	3.069	37.52	60.52

pulses for the strip (N_w) and for each upper surface of the dielectric (N_d). In Table I the c.p.u. time is also given for the program execution on a relatively slow personal computer (IBM PS/2, model 70). The conductor thickness was assumed to be zero, the width of the ground plane was taken to be infinite, but the dielectric width was finite (d). The results of this table clearly show that a much better accuracy is given by nonuniform segmentation than by uniform segmentation, and better accuracy is given by Galerkin's solution than by the point-matching solution, in particular when a small number of sections is used. (Comparisons should be made to the results of Galerkin's method and nonuniform segmentation for $N_w = N_d = 64$, which remain stable with a further increase of N_w and N_d.) This results in a shorter c.p.u. time for a given accuracy by Galerkin's solution than by the point-matching solution, because a smaller number of unknowns is required by Galerkin's method.

In the second example, we illustrate the effect of ground plane width. We consider the microstrip line of Fig. 1 and the stripline of Fig. 2. Given in Table II are the results for the characteristic impedance versus the dimension d. The

TABLE II
INDUCTANCE PER UNIT LENGTH (L'), CAPACITANCE PER UNIT LENGTH (C'), CHARACTERISTIC IMPEDANCE (Z_c) AND EFFECTIVE RELATIVE PERMITTIVITY (ϵ_{re}), OF THE MICROSTRIP LINE OF FIG. 1, FOR $w = 2$ mm, $h = 1$ mm, $\epsilon_r = 4$, AND OF THE STRIPLINE OF FIG. 2, FOR $w = 1$ mm, $h = 1$ mm, AND $\epsilon_r = 4$, VERSUS THE DIMENSION d. FOR BOTH LINES THE FINITE WIDTH OF THE GROUND PLANE IS $2w + d$

		Microstrip line				Stripline
d [mm]	ground plane	L' [nH/m]	C' [pF/m]	Z_c [Ω]	ϵ_{re}	Z_c [Ω]
1	finite	322.8	110.9	53.94	3.219	50.59
1	infinite	297.2	113.1	51.26	3.022	
2	finite	308.5	113.8	52.06	3.156	50.27
2	infinite	297.2	114.8	50.88	3.066	
3	finite	303.5	114.4	51.50	3.122	50.27
3	infinite	297.2	115.0	50.83	3.072	
4	finite	301.3	114.6	51.26	3.104	50.27
4	infinite	297.2	115.1	50.82	3.074	
5	finite	300.0	114.7	51.13	3.094	50.27
5	infinite	297.2	115.1	50.82	3.074	
10	finite	298.0	114.9	50.93	3.078	
10	infinite	297.2	115.1	50.81	3.075	
20	finite	297.4	114.9	50.87	3.072	
20	infinite	297.2	115.1	50.81	3.075	
50	finite	297.3	114.9	50.86	3.071	
50	infinite	297.2	115.2	50.80	3.076	

number of pulses for the strip was 20 for both structures to achieve a high accuracy. The number of pulses for the ground plane was varied in accordance with the width of the ground plane. For example, 150 pulses were taken for the microstrip for $d = 50$ mm, and 15 uniformly distributed pulses were taken for each ground plane of the stripline for $d = 2$ mm. For comparison, the theoretical value for the characteristic impedance of the stripline is 50.25 Ω. These results confirm our recommendations about the ground plane width, given in Section III.

As the last example, we present the results for the multiconductor transmission line sketched in Fig. 3. The thickness of the conductors was taken to be finite in this case (20 μm), they were assumed to be made of copper of conductivity σ =56 MS/m, the loss tangent of both dielectrics was assumed to be 0.001, and the operating frequency was 1 GHz. Other data are given in Fig. 3. The resulting matrices of the primary parameters are obtained to be

$$[L'] = \begin{bmatrix} 282.1 & 47.37 & 28.65 & 8.99 \\ 47.37 & 267.9 & 82.30 & 17.30 \\ 28.65 & 82.30 & 283.9 & 50.54 \\ 8.99 & 17.30 & 50.54 & 290.5 \end{bmatrix} \text{ nH/m},$$

$$[B'] = \begin{bmatrix} 140.4 & -20.52 & -2.29 & -0.47 \\ -20.49 & 157.2 & -32.11 & -0.38 \\ -2.32 & -32.09 & 109.1 & -8.15 \\ -0.47 & -0.38 & -8.16 & 99.69 \end{bmatrix} \text{ pF/m},$$

$$[R'] = \begin{bmatrix} 20.14 & 2.299 & 1.222 & 0.476 \\ 2.299 & 20.38 & 2.614 & 0.550 \\ 1.222 & 2.614 & 12.38 & 1.399 \\ 0.476 & 0.550 & 1.399 & 11.10 \end{bmatrix} \Omega/\text{m},$$

$$[G'] = \begin{bmatrix} 850.0 & -127.0 & -1.2 & 0.1 \\ -126.6 & 951.5 & -177.2 & -0.2 \\ -1.5 & -177.0 & 582.5 & -16.6 \\ 0.1 & -0.2 & -16.6 & 533.7 \end{bmatrix} \mu\text{S/m}.$$

The above results were computed with a total of 213 unknowns. The good symmetry of the above matrices gives a confidence in the accuracy of the results, as in cases of

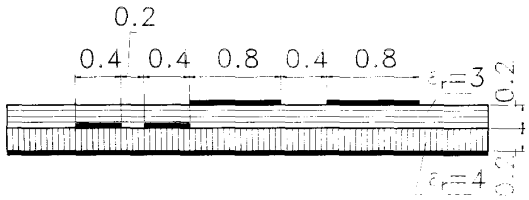

Fig. 3. Sketch of a multiconductor transmission line on a multilayered board. All dimensions are in mm.

a lower accuracy the matrices $[B']$ and $[G']$ become highly unsymmetrical [6].

V. Conclusion

An efficient numerical technique is presented for the evaluation of the primary matrix parameters of multiconductor transmission lines with piecewise-homogeneous dielectrics. The method is based on solving two electrostatic problems, where the distribution of the free and bound charges is obtained as a solution of a system of integral equations using Galerkin's technique with a pulse approximation. The resulting integrals are evaluated in closed forms. As compared to the point-matching method, a significant improvement in accuracy is achieved, together with an increase in efficiency. Guidelines are given about the choice of the pulse distribution, and about the width of the ground plane.

VI. Appendix
Closed-Form Formulas for Field and Potential Integrals

The integrals in (3) and (4) can be evaluated in a closed-form using complex calculus, in a way similar to that used in [12]. It is useful to introduce a local coordinate system (x, y) for the source segment, where the x-axis is along the segment and the segment location is $x \in [-a, a]$.

Let us first evaluate the integral

$$K_{V1}(a, x, y) = -\int_{-a}^{a} \log\sqrt{(x-x')^2+y^2}\, dx', \qquad (8)$$

which, when multiplied by $\rho_{sti}/2\pi\epsilon_o$, yields the potential of the source segment at the field point (x, y). We can set $z' = x' + j0$, and $z = x + jy$. The integration in the complex plane is along the real axis, so that $dx' = dz'$. Then,

$$\log\sqrt{(x-x')^2+y^2} = \mathrm{Re}\{\log(z-z')\}, \qquad (9)$$

since $\log(z) = \log|z| + j\arg(z)$. Note that $\log(z)$ has a branch cut. On most computers $-\pi < \arg(z) \le \pi$, and the branch cut is along the negative part of the real axis. Now,

$$K_{V1}(a, x, y) = -\mathrm{Re}\left\{\int_{-a}^{a} \log(z-z')\, dz'\right\} = \mathrm{Re}\{(z-z')[\log(z-z')-1]\,|_{z'=-a}^{a}\} \qquad (10)$$

The branch cut of the logarithmic function does not have an influence on the final result because only the real part is taken.

The dual integral in (3) has the form

$$-\int_{c_j}\int_{c_i} \log|\vec{r}-\vec{r}'|\, dl'\, dl,$$

where the inner integration (along the source segment c_i) results in $K_{V1}(a, x, y)$. The outer integration is to be taken along the field segment (c_j). We assume that the end points of the field segment are (x_1, y_1) and (x_2, y_2) with respect to the local coordinate system of the source segment, which correspond to $z_1 = x_1 + jy_1$ and $z_2 = x_2 + jy_2$, respectively. We also introduce the unit vector in the direction of the field segment, $\hat{u} = (z_2 - z_1)/|z_2 - z_1|$. The outer integration is carried out in the direction along this unit vector, and $dl = |dz| = \hat{u}^* dz$. Hence, the dual integral in (3) reduces to

$$K_{V2}(a, x_1, y_1, x_2, y_2) = -\mathrm{Re}\left\{\int_{z_1}^{z_2}\int_{-a}^{a} \log(z-z')\, dz'\, \hat{u}^* dz\right\} = \mathrm{Re}\left\{\hat{u}^* \frac{(z-z')^2}{2}\left[\log(z-z') - \frac{3}{2}\right]\Big|_{z'=-a}^{a}\Big|_{z=z_1}^{z_2}\right\}. \qquad (11)$$

The above formula is valid when the field segment has an arbitrary position, including the case when it coincides with the source segment, but not when the field segment intersects the x-axis at $x_o < a$. (The field segment can touch the x-axis if it is in the half-plane $y \ge 0$.) The problem comes from the branch cut, which yields the term $-\mathrm{Re}\{j\pi\hat{u}^*(x_o - a)^2\}$ when $-a < x_o < a$, and $\mathrm{Re}\{4\pi\hat{u}^* x_o a\}$ when $x_o \le -a$, which should be added to the above result.

The electric field at a point (x, y) can be obtained by differentiating $K_{V1}(a, x, y)$ versus x and y. The electric field has two components, and it can be represented as a complex number $E_x + jE_y$, which can be evaluated by multiplying

$$K_{E1}(a, x, y) = \int_{-a}^{a} \frac{1}{(z-z')^*} dz' = -\log(z-z')^*\,|_{z'=-a}^{a} \qquad (12)$$

by $\rho_{sti}/2\pi\epsilon_o$. The real part of the integral has singularities at the end points of the source segment which may be a source of instabilities in the point-matching solution if a matching point is placed close to these points, or in Galerkin's solution if a small field segment is located close to an end point of the source segment. The dual integral in (4) reduces to

$$K_{E2}(a, x_1, y_1, x_2, y_2) = \int_{z_1}^{z_2}\int_{-a}^{a} \frac{1}{(z-z')^*} dz'\, \hat{u}^* dz = -\{\hat{u}^*(z-z')[\log(z-z')-1]\,|_{z'=-a}^{a}|_{z=z_1}^{z_2}\}^*, \qquad (13)$$

since $dz'^* = dz'$ and $\hat{u}dz^* = \hat{u}^* dz$. The contribution of the branch cut must be included in the same cases as for the potential, by adding $[2j\pi\hat{u}^*(x_o - a)]^*$ when $-a < x_o < a$, and $-[4j\pi\hat{u}^* a]^*$ when $x_o \le -a$.

References

[1] T. R. Arabi, T. K. Sarkar, and A. R. Djordjević, "Time and frequency domain characterization of multiconductor transmission lines," *Electromagnetics,* vol. 9, pp. 85–112, 1989.

[2] T. C. Edwards, *Foundations for Microstrip Circuit Design,* Chichester: Wiley, 1981, p. 38.

[3] C. Wei, R. F. Harrington, J. R. Mautz, and T. K. Sarkar, "Multiconductor transmission lines in multilayered and dielectric media," *IEEE Trans. Microwave Theory Tech.,* vol. MTT-32, pp. 439–450, Apr. 1984.

[4] R. F. Harrington and C. Wei, "Losses on multiconductor transmission lines in multilayered dielectric media," *IEEE Trans. Microwave Theory Tech.*, vol. MTT-32, pp. 705–710, July 1984.
[5] J. Venkataraman, S. M. Rao, A. R. Djordjevič, T. K. Sarkar, and Y. Naiheng, "Analysis of arbitrarily oriented microstrip transmission lines in arbitrarily shaped dielectric media over a finite ground plane," *IEEE Trans. Microwave Theory Tech.*, vol. MTT-33, pp. 952–959, Oct. 1985.
[6] M. B. Baždar, A. R. Djordjević, T. K. Sarkar, and R. F. Harrington, *Matrix Parameters for Multiconductor Transmission Lines (Software and User's Manual)*, Boston: Artech House, 1989.
[7] M. B. Baždar, "Evaluation of Matrix Parameters of Multiconductor Transmission Lines by the Galerkin Method," M.Sc. thesis, School of Electrical Eng., Univ. of Belgrade, 1991.
[8] J. R. Mautz, R. F. Harrington, and C. G. Hsu, "The inductance matrix of a multiconductor transmission line in multiple magnetic media," *IEEE Trans. Microwave Theory Tech.*, vol. MTT-36, pp. 1293–1295, Aug. 1988.
[9] R. F. Harrington, *Field Computation by Moment Methods*. New York: Macmillan, 1968. Reprinted by IEEE Press, 1993.
[10] A. R. Djordjević and T. K. Sarkar, "A theorem on the moment methods," *IEEE Trans. Antennas Propagation*, vol. AP-35, pp. 353–355, Mar. 1987.
[11] W. R. Smythe, *Static and Dynamic Electricity*, New York: McGraw-Hill, 1968.
[12] R. F. Harrington, K. Pontoppidan, P. Abrahamsen, and N. C. Albertsen, "Computation of Laplacian potentials by an equivalent-source method," *Proc. IEE*, vol. 116, pp. 1715–1720, Oct. 1969.

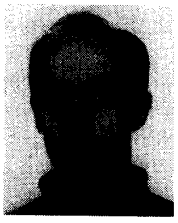

Miodrag Baždar was born in Belgrade, Yugoslavia, on July 30, 1960. He received the B.E.E. and M.Sc. degree from the School of Electrical Engineering, University of Belgrade in 1986 and 1991, respectively. Since 1986 he has been employed in the Institute of Microwave Technology and Electronics in Belgrade, as a research engineering.

Antonije R. Djordjević, for a photograph and biography, see page 249 of the February issue of this TRANSACTIONS.

Roger F. Harrington (S'84–A'53–M'57–SM'62–F'68–LF'92) was born in Buffalo, NY, on December 24, 1925. He received the B.E.E. and M.E.E. degrees from Syracuse University, Syracuse, NY, in 1948 and 1950, respectively, and the Ph.D. degree from Ohio State University, Columbus, in 1952.

From 1945 to 1946, he served as an Instructor at the U.S. Naval Radio Material School, Dearborn, MI, and from 1948 to 1950 he was employed as an Instructor and Research Assistant at Syracuse University. While studying at Ohio State University, he served as a Research Fellow in the Antenna Laboratory. Since 1952, he has been on the faculty of Syracuse University, where he is presently Professor of Electrical Engineering. During the years 1959–1960, he was visiting Associate Professor at the University of Illinois, Urbana; in 1964 he was Visiting Professor at the University of California, Berkeley; and in 1969 he was Guest Professor at the Technical University of Denmark, Lyngby, and in 1983 he was Visiting Professor at the East China Normal University.

Dr. Harrington is a member of Tau Beta Pi, Sigma Xi, the American Association of University Professors, and the International Union of Radio Science.

Tapan K. Sarkar (S'69–M'76–SM'81–F'92), for a photograph and biography, see page 249 of the February issue of this TRANSACTIONS.